Hindawi
Journal of Nanomaterials
Volume 2021, Article ID 6453888, 10 pages
https://doi.org/10.1155/2021/6453888

Research Article

Computed Tomography Imaging Agent Based on Gold Nanoparticles for Internal Iliac Artery Embolization after Endovascular Abdominal Aortic Repair and CCN3 Protection Mechanism

Siying Pei,[1] Yao Sun,[2] Dongxu Fan,[2] Shuhua Deng,[3] Haoran Mei,[2] and Hanrui Wang[2]

[1]*College of Basic Medicine, Jiamusi University, China*
[2]*Department of Vascular Surgery, The First Affiliated Hospital of Jiamusi University, China*
[3]*Nursing Department, Jiamusi Central Hospital, China*

Correspondence should be addressed to Hanrui Wang; whr496196111@163.com

Received 9 April 2021; Revised 12 April 2021; Accepted 16 April 2021; Published 20 May 2021

Academic Editor: Songwen Tan

Abdominal aortic aneurysm is more stressful and has more complications in many diseases. During treatment and repair, arteriosclerosis, abdominal congestion deposition, and abdominal swelling cannot be eliminated. In this paper, we used the seed growth method to obtain gold nanoparticles (AuNPs) with good morphology and dispersion. The AuNPs of larger aspect ratio synthesized in this experiment moved their longitudinal plasmon resonance absorption peak to the near-infrared region, which provided suitable materials for subsequent experiments and laid the foundation for the photothermal therapy of tumors. Experiments show that near-infrared rays can penetrate into deep tissues to overcome the shortcomings that visible light cannot penetrate abdominal aorta well. AuNPs absorb near-infrared rays, thereby generating heat energy to achieve the purpose of treating tumors. In addition, AuNPs also have fluorescent properties, combined with other forms of imaging methods, to achieve the purpose of multimodal imaging, and improve the diagnostic accuracy of studying the protection mechanism of the nephroblastoma overexpressed (NOV or CCN3) gene.

1. Introduction

Abdominal aortic aneurysm (AAA) is defined as a permanent local expansion of the abdominal aorta exceeding 3.0 cm or a diameter exceeding 1.5 times the normal diameter [1], which is a common clinical disease in vascular surgery. According to the survey, 3.9%-7.2% of men and 1.0%-1.3% of women over the age of 50 in the United States may suffer from AAA [2]. The incidence rate increases rapidly with age. 12.5% of men over the age of 50 and 5.2% from 74 to 84 years of women are diagnosed with AAA, and more than 10,000 people die from AAA every year, and the mortality rate of ruptured AAA patients is as high as 90% [3]. The mechanism of AAA is not yet clear. Various factors such as genetic susceptibility, atherosclerosis, and various protease abnormalities may cause it to occur. Various causes will eventually cause degeneration of the middle layer of the aorta, resulting in local permanent blood vessels. The natural course of AAA is closely related to the diameter of the tumor, mainly manifested by the gradual increase of the tumor and the formation of arterial wall thrombosis due to hemodynamic disturbances. The rate of increase in the diameter of the AAA is related to the diameter of the tumor [4]. When the diameter of the AAA tumor is less than 4 cm, the annual diameter increases by about 1-4 mm. When the diameter of the tumor is greater than 5 cm, the diameter increase rate will exceed 5 mm/year. At this time, the tumor rupture rate will reach 20%. If the tumor diameter is greater than 6 cm, the tumor diameter increase rate will further increase to 7-8 mm/year, and the final tumor rupture rate will be as high 40%. Therefore, it is generally considered that tumors larger than 5 cm and women with smaller abdominal aorta

diameters larger than 4.5 cm require surgical treatment. When the size of the tumor grows too fast (>5 mm/half a year) or when the tumor causes pain, it should be timely surgical treatment [5].

Malignant tumors are major diseases that endanger human health. According to the National Cause of Death Survey, the annual mortality rate of malignant tumors in my country is about 10000. Clinical studies have shown that early diagnosis and early treatment are the most effective ways to reduce cancer mortality. Therefore, it is an urgent problem to be solved in the field of biomedicine to strive for new methods of early specific diagnosis of cancer [6]. There are many clinical diagnostic methods for tumors, and imaging is the most widely used clinical examination method. The principle is to differentiate the normal tissue from the diseased tissue according to the different attenuations of rays by different tissues on the image [7]. At present, we commonly used clinical contrast agents including ionic and nonionic, mainly small molecule compounds based on iodine, such as iohexol [8]. However, these small molecule iodine contrast agents have many shortcomings, so the imaging time is short. Lacking of targeting and specificity, it is often accompanied by side effects, with certain renal toxicity. Therefore, the development of multifunctional, high-sensitivity, and high-specificity contrast agents is an effective measure to improve the accuracy of early diagnosis of tumors, and it is also the current development trend of nanomedicine and imaging diagnostics. In recent years, the research on gold nanomaterials has made great progress. People has not only prepared nanoparticles of different sizes but also controlled their morphology and prepared many different shapes of gold nanomaterials. Gold nanoparticles (AuNPs) have unique optical properties. Good biocompatibility and the high atomic number and electron density make it a new potential contrast agent that has attracted wide attention from researchers. The small size of nanoparticles can make the diameter smaller than that of capillaries and thus can enter more tissues [9]. Moreover, due to the enhanced permeability of capillaries in cancerous tissues, nanoparticles can accumulate more in cancerous tissues through leakage, so as to better visualize tumor sites. Because of nonmetal atoms, iodine has good radiation attenuation intensity. Therefore, the contrast agents currently used in the clinic are mainly small molecular compounds based on iodine (such as iohexol). But due to the short imaging time of this small molecular compound, it lacks specificity, and it has certain toxic and side effects on the kidney. Figure 1 shows the schematic process of Au-assisted CT mapping used in abdominal aortic aneurysm. In recent years, experimental studies have shown that the contrast agent based on AuNPs has good contrast effect and can reduce the toxic and side effects of traditional contrast agents [10]. Compared with iodine, gold has a higher atom ordinal number and radiation absorption coefficient. The contrast ratio of gold per unit mass is better than that of iodine, and the modified AuNPs have a longer imaging time and better imaging effect before and after entering the organism [11]. Therefore, using AuNPs for imaging, it is possible to achieve better imaging results at lower radiation doses. With proper functional modification, the targeting and long circulation of gold nanoprobes can be achieved, which can be precise. It shows the tumor morphology, location, and size, with high sensitivity, which can improve the ability of tumor identification and diagnosis. The earliest experiments have confirmed that AuNPs can be used as linear contrast agents [12]. They will be coated with biological phase. Spherical AuNPs (dispersed in buffer) of the capacitive stabilizer were injected into the veins of mice with subcutaneously implanted breast cancer, and then, radiographic imaging was performed using a mammary gland camera. After injection of the gold nanoparticle contrast agent, it could not pass [13]. The blood vessels seen by the rays appear, and even the blood vessels of only the diameter can be seen, and the tumor site can be clearly distinguished [14]. By comparing the contrast effect of the same mass concentration of the iodine contrast agent, it is found that the AuNPs used as contrast agents exhibit a better contrast than iodine contrast. The AuNPs coated with Ryukyu were used for in vivo imaging experiments. It is proved that the coated contrast agent takes longer to develop than the iodine contrast agent [15].

Currently, AuNPs of various shapes, such as gold nanospheres, gold nanowires, gold nanorods, gold nanocages, and gold nanoshells, have been successfully prepared [16]. There are many methods for synthesizing AuNPs, but the "seed" growth method is currently the most widely used synthesis method and is also the method of synthesizing AuNPs in this experiment [17]. The basic principle of the seed growth method is to add a certain amount of gold nanoparticle seed crystals to the reaction solution. By controlling the concentration of the gold seed and the ratio of the growth solution, the directional growth of the gold seed becomes a gold nanorod with a certain aspect ratio. In this experiment, we used the seed growth method to obtain AuNPs with good morphology, and the dispersion of the AuNPs was good. The AuNPs of larger aspect ratio synthesized in this experiment moved their longitudinal plasmon resonance absorption peak to the near-infrared region, which provided suitable materials for subsequent experiments and laid the foundation for photothermal therapy of tumors. In addition, under the same intensity of X-ray irradiation, gold nanoions showed a significant effective analysis intensity and resolution compared to blank samples. Experiments show that near-infrared rays can penetrate into deep tissues to overcome the shortcomings that visible light cannot penetrate the abdominal aorta well. AuNPs absorb near-infrared rays, thereby generating heat energy to achieve the purpose of treating tumors. In addition, AuNPs also have fluorescent properties, combined with other forms of imaging methods, to achieve the purpose of multimodal imaging, and improve the diagnostic accuracy of studying the protection mechanism of CCN3.

2. Materials and Methods

Here, we reviewed the inpatients with surgical diagnosis of AAA from December 2012 to December 2019. Based on medical history, surgical records, and CT image data of preoperative and postoperative review, imaging data and surgery

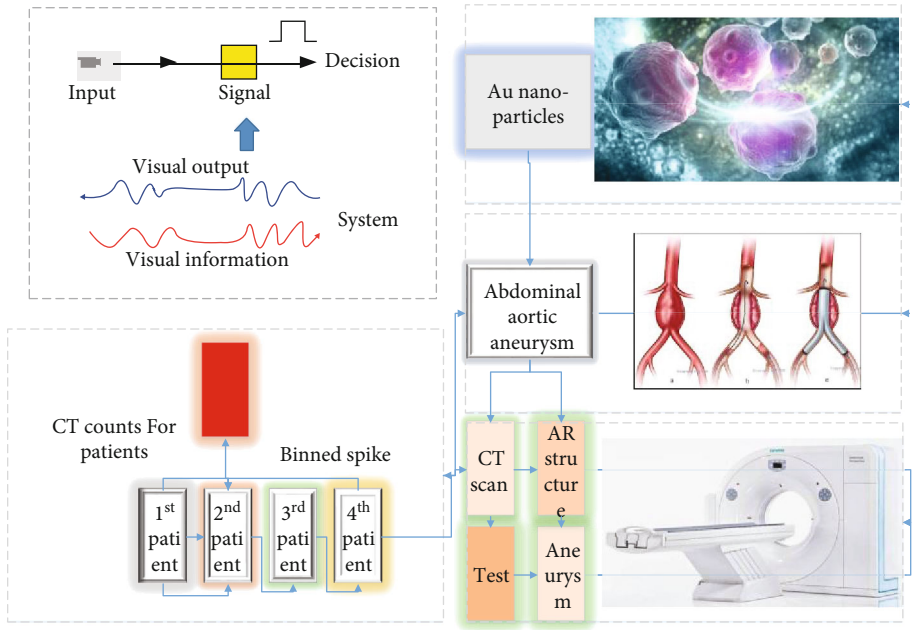

Figure 1: The schematic diagram of Au-assisted CT mapping used in abdominal aortic aneurysm.

showed 32 patients with bilateral internal iliac intact, without stenosis and occlusion. According to the different treatments of intraoperative IIA, they were divided into three groups, namely, the bilateral IIA embolism group, unilateral IIA embolism group, and retained bilateral IIA group. Among them, there were 11 patients in the bilateral IIA embolization group, 9 males and 2 females, aged 66-80 years old, with an average of (73 ± 5) years old. 9 patients were in the unilateral IIA embolization group, 6 males and 3 females, aged 69-89 years old, with an average of (76 ± 6) year. 12 patients were in the bilateral IIA group, all male, aged 34-84 years old, with an average of (62 ± 15) year.The patient was placed in a supine position and routinely sterilized and draped. 32 patients were treated with 2% lidocaine (10 mL/g, Zizhu Pharmaceutical Co., Ltd.). After local anaesthesia, a sharp knife was used to take about 5 mm at the strongest point of bilateral inguinal femoral artery pulsation. The schematic process of patients verified by CT scan can be seen in Figure 2. After skin incision, the bilateral femoral artery was punctured by modified Seldinger's technique [18], and the 6F vascular sheath group (Termo, Japan) was placed. After the same local anaesthesia, the left brachial artery was punctured and the 5F vascular sheath was inserted. The pig tail catheter was inserted into the abdomen. The upper segment of the aorta was monitored by angiography at any time. The black loach guide wire and the 5F gold-labeled pig tail catheter (COOK, USA) were fed through the femoral artery sheath to the level above the bilateral renal artery, and the AAA and peripheral vascular morphologies were observed by angiography. If the patients need to embolize IIA, we insert the Cobra catheter through the vascular sheath and select it to the corresponding IIA, then select the corresponding coil according to the size of the main artery of the IIA (COOK MWCE, United States). After the catheter is inserted into the IIA trunk, embolization is satisfactory. The gold-marked pig tail catheter scale is used as the measurement benchmark to proofread the digital subtraction angiography (DSA) machine (Siemens Artis Zeego, Germany) Leonardo postprocessing workstation measurement tool. After measuring the basic data of AAA, we combine the operation with the mappings. Before the commodity trading advisors (CTA) measurement data, we select the appropriate size stent graft (Medtronic Endurant stent graft system, United States). The femoral artery was sent into the main body stent, and under DSA fluoroscopy, and the main body stent was released at a suitable position in the tumor neck and half released until the contralateral iliac branch was completely released from the tumor cavity. After inserting the guide wire catheter into the aortic iliac branch cavity through the contralateral vascular sheath, the iliac branch stent graft is connected to the external iliac artery, and then, the main body stent is completely released to the common iliac artery or the iliac branch stent is connected to the iliac arteries. After withdrawing the main stent and bilateral femoral artery sheaths, the puncture point was closed with a vascular suture device, and finally, the pig tail catheter indwelling through the brachial artery sheath was subjected to the final angiography. The position of the stent has been clarified, and there is no endoleak. For cases where bilateral IIA is preserved, the process of embolizing IIA is omitted during the operation, and the bilateral iliac branch stent is connected to extend the common iliac artery, retaining the IIA opening.

AuNPs were synthesized in an aqueous solution as follows: first, the gold salt solution is decomposed in an appropriate solution. Second, the gold salt solution is reduced in a certain reducing agent. Finally, the stabilizer synthesis of stable AuNPs was observed. At present, the most popular method for preparing AuNPs is to reduce haucl4 with citrate in the aqueous solution under heating. For this method, by changing the concentration of gold and the concentration

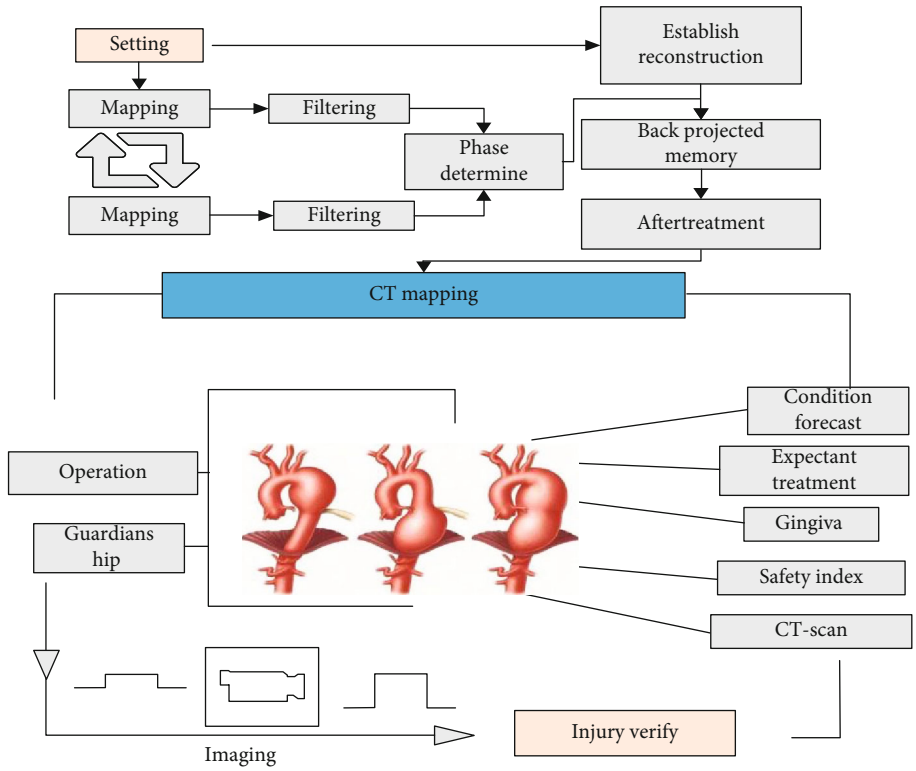

Figure 2: The schematic process of patients verifies by CT scan.

of citrate, a large number of AuNPs with an average particle size (21.8 ± 4.5) nm can be prepared.

3. Results

3.1. Endoluminal Repair of Abdominal Aortic Aneurysm Embolizes Internal Iliac Artery Circulation. The unilateral internal iliac embolism group is slightly older than the bilateral internal iliac embolism group, and the retention of the bilateral internal iliac group is relatively young. The AAA classification composition ratio between the three groups is large, and the bilateral internal iliac embolism group is type IIC [19]. Mainly, while the unilateral internal iliac embolism group is mainly type IIB, and the number of cases of AAA type IIA and type IIB of the bilateral internal iliac group is about the same. The maximum tumor diameter of AAA between the three groups is not much different. The pelvic ischemic complications only appeared in the bilateral internal iliac embolism group in this study 20]. The 4 cases of pelvic ischemic complications were mainly gluteal muscle ischemia, and all patients complained of a little soreness on the buttocks on the first day after surgery. When walking, the aggravation of gluteal muscle avascular necrosis and intestinal ischemia was absent. One week after the operation, the four patients had basically relieved the symptoms of gluteal muscle ischemia before discharge and complained of no obvious hip pain and discomfort after walking for about 500 meters. Two cases of type II endoleak caused by reflux after internal iliac artery embolization were found in the double-stage IIA embolization group after CT review. Currently, two cases of type II endoleak are under follow-up. The patient has no complaints, and the CT review image is not seen. Type II endoleaks increase and do not require intervention. The secondary intervention occurred in the bilateral IIA occlusion group. Here, we use Au nanoparticles to enhance the ion diffusion. And Figure 3 shows the functions of the Au nanoparticles in the ion passage and drug effect. When a blood vessel is severely narrowed or occluded, the potential anastomotic vessels present in the surrounding tissue of the blood vessel will supply open blood flow to the ischemic area, manifesting as the surrounding branch vessels to the anastomotic vessels gradually thicken and the blood flow gradually increases. The function of the original ischemic area is restored and free from necrosis. This pathophysiological change is called collateral circulation, which is an endogenous bypass vascular network that exists in most tissues. It is open during occlusion and ischemic injury. The collateral circulation can be an arterial-arterial connection or a connection of new microcirculation small vessels, which most intuitively represents the increase in the diameter of these collateral circulation blood vessels.

The establishment of collateral circulation also occurred after ethylene vinyl acetate (EVAR) embolization IIA. In order to clarify this result, pelvic blood vessels were involved in this process after embolization IIA. This study selected theoretically the most complete pelvic ischemia bilateral IIA embolism group and pelvic ischemia. The comparatively lighter unilateral IIA embolization group preoperative and postoperative CTA images were used as a comparison, and the changes in the diameter of the pelvic vessels before and after the operation in this group of patients were measured. At the same time, the pelvic vessels before and after the

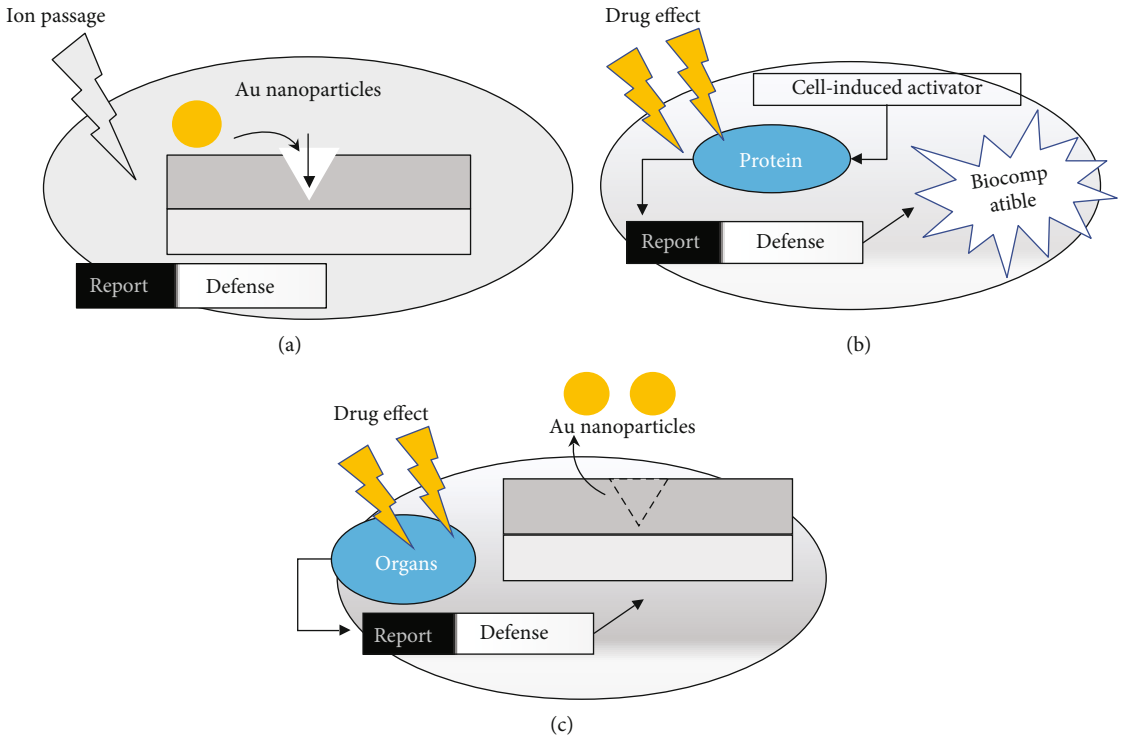

Figure 3: The functions of the Au nanoparticles in the ion passage and drug effect.

operation in the bilateral IIA group were retained as a comparison reference. It takes time to establish the collateral circulation, which depends on various factors such as the patient's age, vascular conditions, circulation status, and exercise status. In this study, 4 patients in the bilateral IIA embolism group developed pelvic ischemic symptoms and dilated blood vessels. The symptoms can be significantly alleviated, and the patients complained of basically relieved symptoms within 1 week after surgery and then were approved for discharge and continued to take oral cilostazol and beraprost sodium to improve circulation and prevent symptom recurrence. We considered that the relief of pelvic ischemic symptoms in these 4 patients is related to the eventual establishment of collateral circulation and considered transient gluteal muscle ischemia, so these 4 patients were included in this study. It is reported that observation of collateral circulation arterial models in the dogs' and pigs' hearts, rabbit hind limbs, mouse hind limbs, and other collateral circulation arteries is generally well established after 3 weeks to 5 weeks after operation, so this study selected patients from 3 months to 6 months after surgery. The CT images of the postoperative review were used as observation objects to obtain good observation of collaterals and control the influence of time variables on collateral circulation.

In this study, first, the two attending physicians carefully reviewed the postoperative CT images of patients in the bilateral IIA embolization group and the unilateral IIA embolization group and recorded the blood vessels that participated in the blood supply to the pelvic organs and muscle groups after surgery as shown in Figure 4. The observable blood vessels were the inferior mesenteric artery, inferior abdominal wall artery, deep circumflex iliac artery, superficial iliac artery,

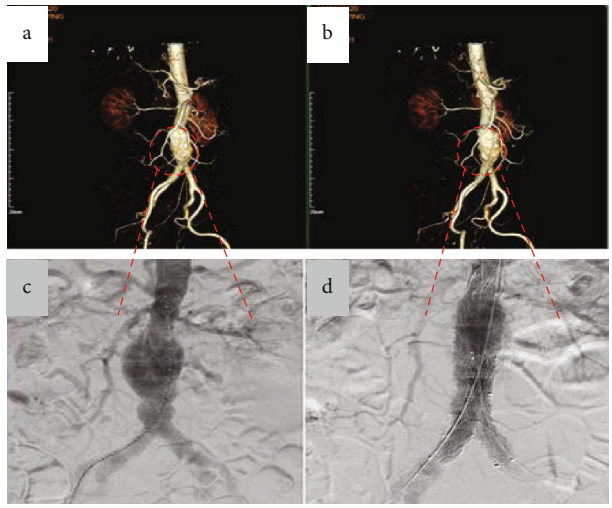

Figure 4: The CT mapping of the patients in the bilateral IIA embolization group and the unilateral IIA embolization group. The letters a and c indicate the bilateral IIA embolization group and the letters b and d indicate the unilateral IIA embolization group.

external pudendal artery, medial femoral artery, ascending branch of lateral femoral artery, and median sacral artery. From the baseline information in this group of AAA patients, it can be seen that most AAA patients have risk factors associated with hypertension, heart disease, smoking history, etc., and there is a high possibility of vascular sclerosis and occlusion. The vascular wall sclerosis of AAA patients is often very serious, so the abovementioned blood vessels may slowly occlude in the process of vascular wall sclerosis as the age

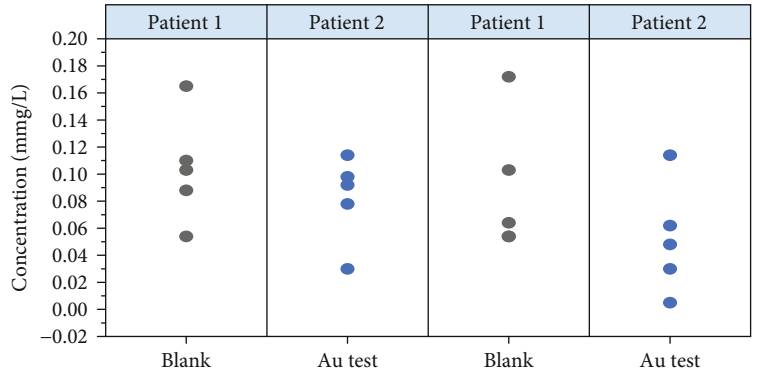

Figure 5: The concentration of AuNPs in the patients.

and time of the patient increase. If EVAR is used to embolize and close IIA, the muscles and organs of the pelvic area need to rely on the abovementioned blood vessels to maintain blood supply. It can be seen from the CTA images of this group of patients that only 2 were detected in the unilateral sacral median artery embolization group and bilateral embolism group after embolization of IIA in this group of patients. While in the two groups for the subabdominal artery and inferior mesenteric artery, the detection rate is 100% in both. The detection rate, the medial circumflex femoral artery, and the ascending branch of the lateral circumflex femoral artery are more than 80% in both groups. The detection concentration of the external pudendal artery and superficial circumflex iliac artery are mostly hovering between 0.02 mmg/L and 0.20 mmg/L. Only lateral pudendal arteries were detected in the Au test group (Figure 5).

In this study, the diameter of the abovementioned arteries in the group was significantly thicker than before the operation, and P was less than 0.05. When comparing the differences in blood vessels before and after the IA group on both sides, the diameter of the corresponding blood vessels after the operation, except under the abdominal wall, was almost equal to the diameter of the blood vessels before the operation. Outside the artery, the P value is greater than 0.05 and the average diameter of the blood vessels before and after the pancreas makes no significant difference in this group and has no apparent clinical significance. This means that the two-sided IIV embryo group is better than the two-sided IIA group. The ascending branches of the lateral rotary artery are significantly thicker than the corresponding blood vessels, preoperative CTA. Further, embryos of the bilateral IIA group and the retention of the bilateral IIV, in the bilateral IIA group after the mean metabolism of the CTA blood vessels at the pose, the lower abdominal standard, deep intestinal martyrdom, the internal femoral artery, and the ascending branches of the external femoral artery were significantly thicker than the bilateral IIA group obtained. Statistically speaking, the P value was below 0.05. The lower mesentery, surface, and vulgarity series were statistically insignificant between the two groups, and the P value was greater than 0.05. The branch of the internal intestinal martyrdom is mainly divided into branches of the walls and branches of the internal organs. The branches of the wall nourish the pelvis and external muscle groups such as closed muscle arteries,

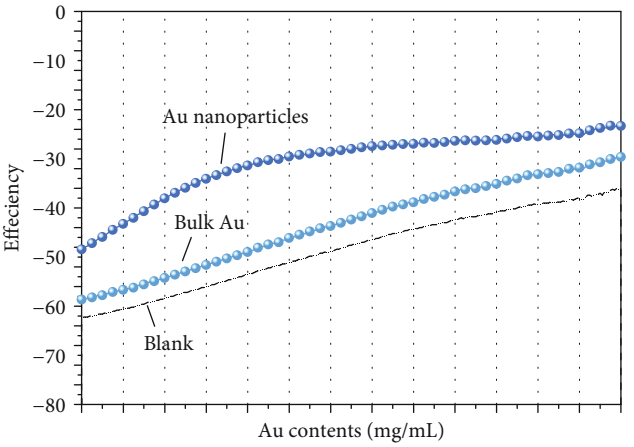

Figure 6: The effects of different states of AuNPs and blank tests.

upper enteral arteries, lower enterus arteries, enteric tendon arteries, and lateral sacral arteries. Nutrients for pelvic and outer genital gluteus muscle, including the upper bladder artery, lower bladder artery, lower rectal artery, and inner pubic region, are mainly supplied by upper and lower buttock arteries. The upper entrance is divided into deep branches and flat branches, and flat branches reach from the back of the main hall to the main hall and provide the main hall as shown in Figure 6, Au bulk runs deep through the middle gluten muscle and is delivered to the middle gluten muscle, and au nanoparticles are delivered mainly to the lower part of the main hall and the back of the thigh bone. The lower buttocks and distal parts are also first derived from the outer femoral artery. The perforated artery is supported by the ascending branch, and the closed artery is divided into the front and back branches. The front branch corresponds to the inner branch, and the femoral artery and the rear branch correspond to the imperial artery. Shameful branches of the pubis are anastomy. Reticular bowel martyrdom is mainly divided into the intestinal muscle branches, intestinal branches, abdominal wall branches, mainly intestinal muscles, intestinal bones, abdominal blood supply, and deep branches of upper hip, and fourth tendon arteries.

Side valve vessels that have anaesthetic branches and are directly connected to the upper and royal arteries, or are

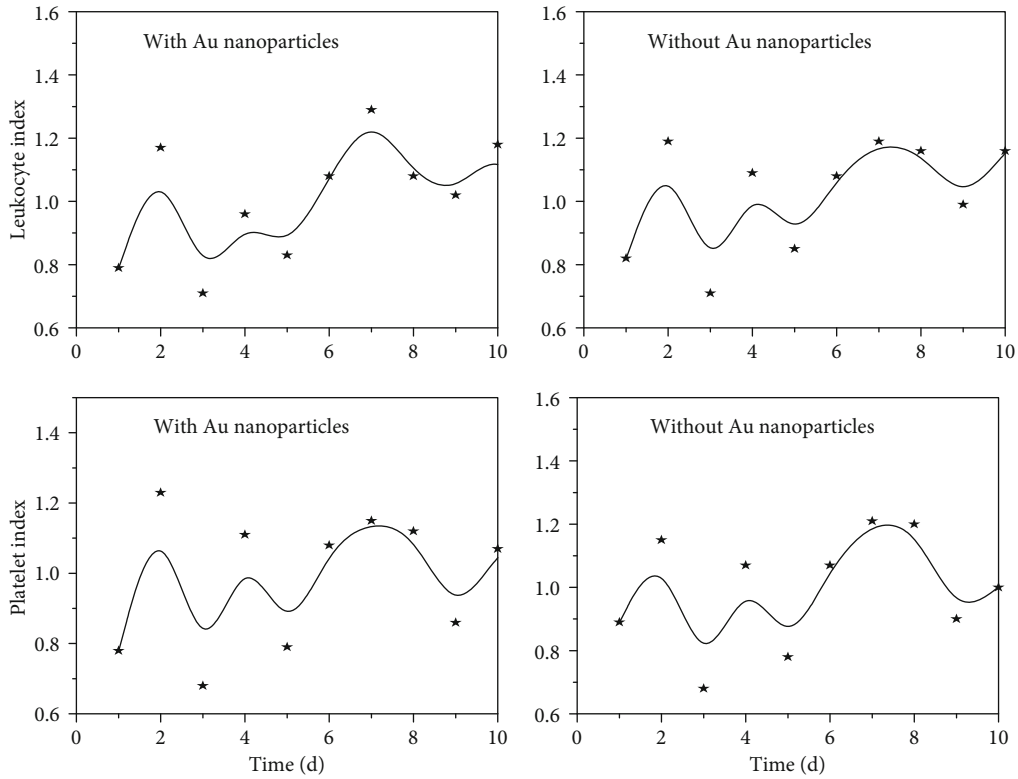

Figure 7: The platelet index and leukocyte index of CCN3 in the presence and absence of AuNPs.

delivered directly to parts of the buttocks, the upper branches of the outer femoral artery, the deep intestinal artery, and the anastomy are transferred to the lower intestines: the abdominal parameter. The supply of distal muscles is an important guarantee for the blood supply of the buttock muscle after the internal enteric artery embolism by EVAR. In summary, the IIA on both sides of the EVAR embryo, the lower abdominal artery, the deep intestinal martyrdom, the inner thigh artery, and the lateral thigh artery may be lateral circulatory vessels of the buttock muscle, preventing cervical muscle ischemia after surgery. This has an important remuneration function. In order to determine the unavoidable EVAR of Embolia IIA, the lower abdominal artery, the deep intestinal artery, the inner thigh artery, and the lateral rotational femoral artery after the preoperative CTA are preoperative. The opening is narrow and small, and the ascending branches of the lower building charterie, the deep intestinal artery, the inner thigh artery, and the outer thigh artery can be completely supplemented to predict the possibility of postoperative cervical ischemia. The blood supply of the bladder is abundant and includes mainly bladder branches of the upper, middle, and lower bladder arteries, vassals and uterine arteries, vaginal arteries, closed arteries, and royal arteries. The blood supply of the prostate is also relatively plentiful, especially twice. In the internal sham artery, lower rectal artery, and lower bladder artery branch, prostate artery from the lower bladder artery is the most important. From the blood supply of the uterus and its accessories comes above all: bilateral uterine arteries and their branches, and abdominal aorta are shared directly. The blood supply of the perineum and the penis is mainly obtained from the bilateral internal sham artery and its branches. An S-shaped colon is obtained mainly from the Si-shaped double-percussion artery submersion. It forms a high anastomy in the descending branches of the left double artery and a low anastomy in the rectal artery. The blood supply of the rectum includes the lower mesentery artery, the subcutaneous artery from the branches of the middle colon, the inner enteric artery, and the lower rectal artery of the inner chambers. There is a lot of anastomy between these three blood vessels. It can be seen that the blood source of the pelvic organ is relatively complex. The anaesthesia between them is the anastomy of the pelvic ganglia and is basically the anastomy of the visceral branches IIA and a lack of potential communication between the vascular branches and the vascular branches of the intestinal tract. If the internal intestinal martyrdom is embolism or blocked, the blood supply of the internal branch of intestinal martyrdom is mainly redistributed to the branches of the internal intestinal system and the lower mesenteric artery of the inverse blood flow of the lateral accompanying vessels of the external enteric artery and the femoral artery. Arteries and other blood vessels are connected to branches of the internal intestinal system and can reach a wide range of the pelvis. Organs can receive a blood supply. This may be the reason why there are relatively few ischemic complications associated with the embolism of the internal intestinal organs.

3.2. CCN3 Protection Mechanism. The study found that the abdominal aortic aneurysm tissue has four main characteristics: immune cells invade the blood camp wall, increased

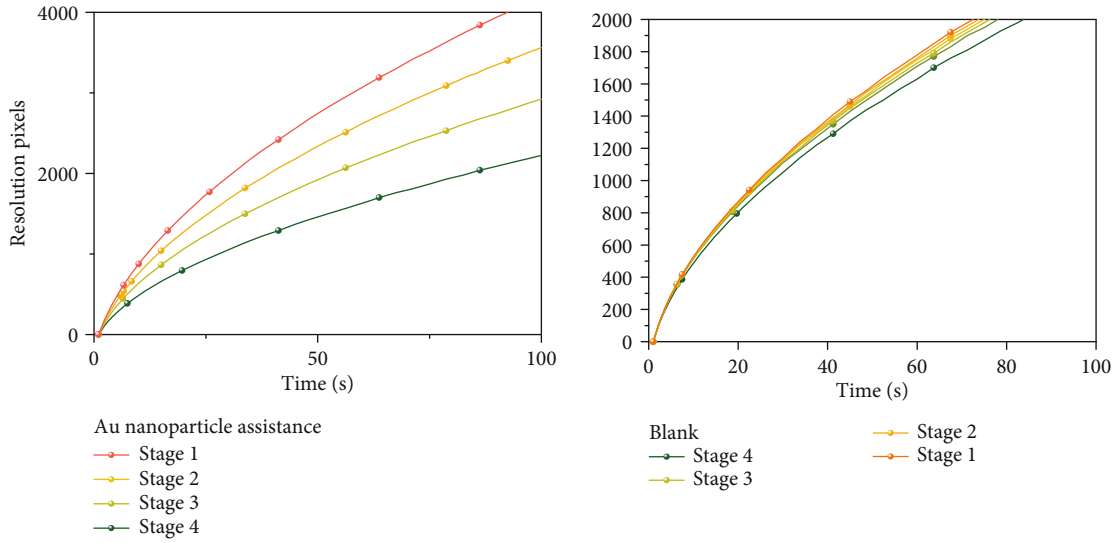

Figure 8: The resolution pixels in different stages.

matrix proteinase activity, destruction of elastin and collagen in the middle and outer layers of the blood vessel, and remodeling of the blood vessel matrix. From the perspective of a pathogenic mechanism, abdominal aortic aneurysm is the result of the interaction of vascular smooth muscle cell apoptosis, enzymatic abnormalities, and inflammation. It is currently known that multiple risk factors are associated with abdominal aortic aneurysms. Family history is positively correlated with the occurrence of abdominal aortic aneurysms. Plasma levels and blood glucose levels are negatively correlated with abdominal aortic aneurysms-6. In view of the serious consequences of the rupture of abdominal aortic aneurysms and the complexity of the etiology, it is particularly important to further study its pathogenesis. CCN3 protein is an extracellular matrix signal-related protein, which has the function of signal regulation and transmission, and belongs to the CCN protein family. This protein family has six structurally similar members, of which CCN3 is also known as N0V. In recent years, studies have found that CCN3 has a wide range of physiological functions and is involved in regulating blood stem cell hyperplasia 7, hepatocyte fibrosis, tumor angiogenesis, bone regeneration, fibrosis, fibrosis, cancer, and other physiological and pathological processes. CCN3 has four protein binding sites, which can combine different ligands to exert different signal regulation effects. Previously, our experimental group found that CCN3, as an extracellular signaling protein, can regulate endothelial cell inflammation and inhibit inflammation factors. Expressed in vascular diseases, inflammation of endothelial cells is an important part of disease occurrence, such as arteritis, atherosclerosis, and deep vein thrombosis. In our early experiments, we fed with a high-fat diet. We later found that atherosclerosis was significantly increased (unpublished). Based on the vascular inflammation regulation of CCN3, we speculate that CCN3 may be involved in regulating the pathogenesis of abdominal aortic aneurysms.

We tested human and mouse abdominal aorta with and without Au nanoparticles. The expression of CCN3 in the platelet index and leukocyte index was changed, and it was found that the expression of CCN3 was reduced as shown in Figure 7. Using the CCN3 gene knockout mouse abdominal aortic aneurysm model, it was found that the lack of CCN3 has the effect of promoting the development of abdominal aortic aneurysm. After analysis, it was found that ERK1/2 was derived from the blood vessels. The abnormal activation of the extracellular lunar, extracellular signal-regulated kinase 1/2, and the signaling pathway are induced by CCN3-deficient mice. After blocking the ERK1 signaling pathway by genes and drugs, W and drugs blocked the production of ROS and successfully inhibited the occurrence of abdominal aortic aneurysms in CCN3 mice. Based on the above results, we conclude that CNN3 exerts its ability to inhibit vascular inflammation by regulating the generation of the ERK signaling pathway and ROS role. In the study of the mechanism of aneurysms, the excessive activation of the Angl-ATIR and classic and nonclassical TGF-B signaling pathways leads to abnormal activation of vascular inflammation signaling pathways and enhanced inflammation. As shown in Figure 8, when inflammation-related signaling pathways are activated in stages 1 and 2, the resolution pixels of cells such as fibroblasts and smooth muscle cells secrete a ratio of 6 using Au NPs compared to the blank group. CCN3 protein has a wide range of physiological functions, involved in regulating cell proliferation, hepatocyte differentiation, and tumor blood vessels. We revealed that CCN3 regulates vascular endothelial inflammation by inhibiting NF-κB signaling pathway plays a protective role in inflammation. In view of the important role of endothelial cells in the regulation of vascular function, we speculate that CCN3 has a regulatory role in vascular inflammatory diseases such as abdominal aortic aneurysms.

4. Discussion

Reviewing the CTA pelvic vascularity of 4 patients with gluteal muscle ischemia after embolizing bilateral IIA in this

study, the 4 patients had severe calcification of abdominal aorta and iliac arteries, aged 73-80 years, with an average of (77 ± 3) years. In the bilateral internal iliac artery embolization group, it is relatively older, although there were preoperative and inferior abdominal wall arteries, deep iliac arteries, medial femoral artery, and ascending branch of lateral femoral artery. The superficial iliac artery is basically present. The corresponding blood vessels also thickened at 3 months after surgery. Comparing with other patients without gluteal muscle claudication in the bilateral internal iliac embolism group, no significant difference was found in CTA images before and after surgery. But according to literature reports, age is a predictor of claudication of gluteal muscles and the 4 patients having a higher age have more vascular plaques. And the other 2 patients have a history of diabetes, hypertension, and chronic renal insufficiency. It is also a factor we fully consider before deciding whether to embolize the internal iliac artery before surgery. For AAA patients with unilateral embolization IIA, one side IIA is preserved during EVAR to ensure blood supply to one pelvic organ and muscle group, and there is an extensive collateral circulation communication between the two sides of IIA, which makes pelvic ischemia complicated. The incidence of morbidity was significantly reduced. In this study, the unilateral IIA embolization group had no pelvic ischemic complications and had a lower incidence of endoleaks than the bilateral IIA embolization group. Further analysis of thin layer CT data in combination with VR vascular reconstruction technology makes it possible to find communication patterns between the pelvic and pelvic regions and muscle groups according to embolis IIA (e.g., the main stem of the lower mesenteric artery) by EVAR surgery. In a group of patients having 100%, the mesentery artery and the superior mesentery artery side subcommunication was observed. The arch of the artery, which mainly has an important communication branch between the upper mesentery artery and the lower mesentery artery, is an important communication branch. In general, the limbic arterial arch is relatively thin. The Rioran artery arch is relatively thick and frequent. The presence of these two important branches opens the lower mesentery artery when the opening is blocked and avoids the occurrence of intestinal ischemia. The closure stop geometry has a wide range of anaesthetic branches in the pool, and after the literature, there is the possibility of an anaesthetic branch with the medial femoral artery, the lower abdominal standard, and the flat branches of the opposite IIA. This group of patients is particularly patients with bilateral intraeal osteoedema. Abdominal abnormalities, medial rotational femoral arteries, vulcanic arteries, and closed arteries are associated with the IIA vulva artery branches, where lower abdominal and medial rotation femoral arteries are more common. In addition, the deep retheral artery is transferred through the anastotic branch on the surface of the lithium orbit to the upper enterus, and the upper branch of the outer rotational femoral artery is transferred through the lower hip branch to the branch of the imperial artery. The use of the IIA branch on the emboli side facilitates communication and promotes the connection of the secondary monitoring circulation and the construction of the above-mentioned vessel networks. Therefore, if the IA embolism is unavoidable in EVAR, you must select the IA progenitor embolism to minimise the effect of IIV on distal blood vessels, containing no branches of IGE. This is the same as IIA stem embolism. Compared to peripheral asthma embolism, the risk of pelvic ischemia is lower. In combination with the lateral collateral pathway connecting to the enteric artery embolism mentioned above, the preoperative CTA assesses the complete presence of the lower abdominal standard, the medial femoral artery, the deep intestinal artery, and the outer femoral artery. Since the stem contains no branches, the lower abdominal standard, the medial rotary artery, the deep ileum artery, and the lateral rotational femoral artery to the side branches of the IIA branch are relatively safe insurgery, which is not affected by embryoorism.

Accurate and controllable observation and analysis of intra-abdominal internal arterial circulation have become the focus and difficulty of treating abdominal aortic aneurysms. Among them, nanogold ions have strong absorption of X-rays at low dimensions and have local plasma resonance effect in the near ultraviolet band, which can significantly enhance the CT image signal. In this paper, we used the seed growth method to obtain AuNPs with good morphology and good dispersion of gold nanogold. The AuNPs of larger aspect ratio synthesized in this experiment moved their longitudinal plasmon resonance absorption peak to the near-infrared region, which provided suitable materials for subsequent experiments and laid the foundation for photothermal therapy of tumors. In addition, under the same intensity of X-ray irradiation, gold nanoions showed significant effective analysis intensity and resolution compared to blank samples. Experiments show that near-infrared rays can penetrate into deep tissues to overcome the shortcomings that visible light cannot penetrate the abdominal aorta well. AuNPs absorb near-infrared rays, thereby generating heat energy to achieve the purpose of treating tumors. In addition, AuNPs also have fluorescent properties, combined with other forms of imaging methods, to achieve the purpose of multimodal imaging, and improve the diagnostic accuracy of studying the protection mechanism of CCN3.

Data Availability

The data used to support the findings of this study are included within the article.

Ethical Approval

All data, models, and code generated or used during the study appear in the submittal complying With Ethics of Experimentation Statement. The study follows the principles of the Declaration of Helsinki.

Conflicts of Interest

The authors declare that they have no conflicts of interest.

Authors' Contributions

Siying Pei and Yao Sun contributed equally to this work and should be considered as coauthor.

Acknowledgments

The authors acknowledge the Funding of Mechanism of Notch signaling pathway on angiogenesis in diabetic rats (Grant: 2018-KYYWF-0967).

References

[1] N. Sakalihasan, R. Limet, and O. D. Defawe, "Abdominal aortic aneurysm," *Lancet*, vol. 365, no. 9470, pp. 1577–1589, 2005.

[2] E. Lindvall, J. Davis, A. Martirosian, G. Garcia, and L. Husak, "Bilateral internal iliac artery embolization results in an unacceptably high rate of complications in patients requiring pelvic/acetabular surgery," *Journal of Orthopaedic Trauma*, vol. 32, no. 9, pp. 445–451, 2018.

[3] H. Shan, A. Padole, F. Homayounieh et al., "Competitive performance of a modularized deep neural network compared to commercial algorithms for low-dose CT image reconstruction," *Nature Machine Intelligence*, vol. 1, no. 6, pp. 269–276, 2019.

[4] D. I. Tsilimigras, F. Sigala, G. Karaolanis et al., "Cytokines as biomarkers of inflammatory response after open versus endovascular repair of abdominal aortic aneurysms: a systematic review," *Acta Pharmacologica Sinica*, vol. 39, no. 7, pp. 1164–1175, 2018.

[5] G. Dovell, C. A. Rogers, R. Armstrong, R. A. Harris, R. J. Hinchliffe, and R. Mouton, "The effect of mode of anaesthesia on outcomes after elective endovascular repair of abdominal aortic aneurysm," *European Journal of Vascular and Endovascular Surgery*, vol. 59, no. 5, pp. 729–738, 2018.

[6] G. Giordano, D. Meo, and M. S. Lio, "Internal iliac artery aneurysm embolization with direct percutaneous puncture and thrombin injection," *Radiology Case Reports*, vol. 15, no. 3, pp. 210–213, 2020.

[7] Q. Yang, P. Yan, Y. Zhang et al., "Low-dose CT image denoising using a generative adversarial network with Wasserstein distance and perceptual loss," *IEEE Transactions on Medical Imaging*, vol. 37, no. 6, pp. 1348–1357, 2020.

[8] P. Kjellin, H. Pärsson, and H. I. V. Lindgren, "Onyx embolization for occlusion of the proximal internal iliac artery during EVAR in patients with unsuitable landing zones in the common iliac artery," *Cardiovascular and Interventional Radiology*, vol. 42, no. 7, pp. 956–961, 2019.

[9] F. A. Lederle, T. C. Kyriakides, K. T. Stroupe et al., "Open versus endovascular repair of abdominal aortic aneurysm," *The New England Journal of Medicine*, vol. 380, no. 22, pp. 2126–2135, 2019.

[10] V. T. le, V.-C. Nguyen, X.-T. Cao et al., "Highly effective degradation of nitrophenols by biometal nanoparticles synthesized using Caulis spatholobi extract," *Journal of Nanomaterials*, vol. 2021, Article ID 6696995, 11 pages, 2021.

[11] J. Beik, M. Jafariyan, A. Montazerabadi et al., "The benefits of folic acid-modified gold nanoparticles in CT-based molecular imaging:radiation dose reduction and image contrast enhancement," *Artificial Cells Nanomedicine and Biotechnology*, vol. 46, no. 8, pp. 1993–2001, 2017.

[12] V. T. Huong, N. T. T. Phuong, N. T. Tai et al., "Gold nanoparticles modified a multimode clad-free fiber for ultrasensitive detection of bovine serum albumin," *Journal of Nanomaterials*, vol. 2021, Article ID 5530709, 6 pages, 2021.

[13] T. F. X. O'Donnell, L. T. Boitano, S. E. Deery et al., "Open versus fenestrated endovascular repair of complex abdominal aortic aneurysms," *Annals of Surgery*, vol. 271, no. 5, pp. 969–977, 2020.

[14] R. A. Stokmans, P. P. H. L. Broos, M. R. H. M.v. Sambeek, J. A. W. Teijink, and P. W. M. Cuypers, "Overstenting the hypogastric artery during endovascular aneurysm repair with and without prior coil embolization: a comparative analysis from the ENGAGE Registry," *Journal of Vascular Surgery*, vol. 67, no. 1, pp. 134–141, 2018.

[15] G. Courtois, M. E. Makrygiannis, R. Hachemi et al., "Positron emission tomography/computed tomography predicts and detects complications after endovascular repair of abdominal aortic aneurysms," *Journal of Endovascular Therapy*, vol. 26, no. 4, pp. 520–528, 2019.

[16] A. Pandey, S. Khadka, and Y. Wan, "Hydroxyethyl starch-based functionalization of gold nanorods: a possible alternative to polyethylene glycol as a surface modifier," *Journal of Nanomaterials*, vol. 2021, Article ID 5555448, 11 pages, 2021.

[17] X. Zheng, S. Ravishankar, Y. Long, and J. A. Fessler, "Pwls-Ultra: an efficient clustering and learning-based approach for low-dose 3d CT image reconstruction," *IEEE Transactions on Medical Imaging*, vol. 37, no. 6, pp. 1498–1510, 2018.

[18] Y. Han, D. Wu, A. Sun et al., "Selective embolization of the internal iliac arteries for the treatment of severe hemorrhagic cystitis following hematopoietic SCT," *Bone Marrow Transplantation*, vol. 41, no. 10, pp. 881–886, 2008.

[19] P. Kulig, K. Lewandowski, B. Banaś, P. Piekorz, A. Kostka, and M. Zaniewski, "Short-term outcomes of endovascular repair of abdominal aortic aneurysm, including ruptured cases," *Videosurgery and Other Miniinvasive Techniques*, vol. 13, no. 2, pp. 243–249, 2018.

[20] M. Ripepi, G. Varetto, L. Gibello, M. A. Ruffino, P. Fonio, and P. Rispoli, "Successful percutaneous transgluteal embolization of a complex arteriovenous malformation feeding a hypogastric artery aneurysm," *Journal of Vascular Surgery Cases and Innovative Techniques*, vol. 4, no. 1, pp. 45–49, 2018.